Effect of different iron concentrations on growth, lipid accumulation, and fatty acid profile for biodiesel production from *Tetradesmus obliquus*

Houman Rajabi Islami [1] · Reza Assareh [2]

Abstract

The present study investigated the effect of ferric iron on growth and lipid content of the green microalga *Tetradesmus obliquus* as a promising feedstock with favorable features for biodiesel production. The microalga was isolated from a freshwater body and cultured for 20 days in five types of modified BG11 medium with different concentrations (0, 10^{-4}, 10^{-3}, 10^{-2}, 10^{-1} mmol L^{-1}) of ferric iron. The algae grown in medium supplemented with 10^{-2} mmol L^{-1} ferric iron had the highest specific growth rate of 0.36 $\pm$ 0.04 day^{-1} and remained in the exponential growth phase over the next 6 days compared with those grown in medium without iron supplementation. The peak of lipid content (34.19 $\pm$ 1.93% dry weight, DW) and biomass productivity (459.20 $\pm$ 2.37 mg L^{-1} day^{-1}) was obtained in the media supplemented with 10^{-2} and 10^{-1} mmol L^{-1} ferric iron, respectively. The highest proportion of saturated fatty acids and the lowest proportion of unsaturated fatty acids were also achieved by adding 10^{-1} mmol L^{-1} ferric iron to the growth medium. These findings may lead to a two-step process for lipid production from *T. obliquus*, in which biomass should be separated from the culture supplemented with 10^{-2} mmol L^{-1} ferric iron concentration to achieve the maximum algal biomass in the first step and then inoculated to the culture supplemented with 10^{-1} mmol L^{-1} ferric iron concentration to reach the highest lipid productivity in the second step, leading to optimization of lipid production from *T. obliquus*. Although the quality of biodiesel produced from *T. obliquus* met the specification of the European biodiesel standard (EN14214) in all media, ferric iron supplementation could be used to optimize the lipid characteristics of *T. obliquus* for biodiesel production.

Keywords *Tetradesmus obliquus* · Chlorophyceae · Ferric iron · Fatty acid profile · Biofuel

Introduction

Global warming due to the accumulation of greenhouse gases in the atmosphere as well as diminishing world oil reserves owing to both mechanized transportation and large-scale industrialization has drawn a substantial attention to search for alternative sources of energy with higher environmental and economic sustainability (Borowitzka and Moheimani 2013; Shuba and Kifle 2018). Biodiesel, monoalkyl esters of vegetable oils or animal fats, is a renewable, clean burning fuel that

is expected to offer new opportunities to overcome energy shortage in different countries, especially those lacking conventional fuel resources (Mata et al. 2010). Biodegradability, renewability, sustainability, and extensive obtainability followed by the environmentally desirable and economically feasible properties are some unique features making biodiesel an excellent alternative for petroleum fuels. Soybean oil is currently the major feedstock for production of biofuel, while other sources like canola oil, palm oil, corn oil, animal fats, jatropha oil, and even restaurant wastes are less important for commercial production (Borowitzka 1992; Chisti 2007; Rodolfi et al. 2009; Demirbas 2011).

In spite of many advantages, biofuel production from crop sources has several obstacles for widespread use as a substitute for petroleum-derived fuel, among which competition with other agricultural activities for exploitation from limited arable lands and the considerable upward pressure on food prices due to the increasing demand for food crops grown for biofuel production are the most important ones (Lang

✉ Houman Rajabi Islami
rajabi.h@srbiau.ac.ir; houman.rajabi@yahoo.com

[1] Department of Fisheries, Science and Research Branch, Islamic Azad University, P.O. Box: 14515-775, Tehran, Iran

[2] Young Researchers and Elite Club, North Tehran Branch, Islamic Azad University, Tehran, Iran

et al. 2001; Patil et al. 2008; Ahmad et al. 2011). Accordingly, several attempts have been made to identify new biomass sources for production of renewable energy in the form of biodiesel. Microalgae are the major photosynthetic primary producers at the basis of food chains that have recently received a lot of attention as a renewable feedstock to meet global demand for energy supply. Appropriate growth rate, widespread availability, high photosynthetic efficiency, and relatively high oil yields along with their high carbon dioxide consumption have made microalgae exceptional candidates for biofuel production compared with the other energy crops (Chisti 2007; Amaro et al. 2011; Koller et al. 2014; Salamaa et al. 2017).

Under favorable growth conditions, most algae convert solar energy via photosynthesis to value-added products like fatty acids which are principally used as substrates for esterification into membrane lipids (Hu et al. 2008). However, unfavorable conditions like stress change this biosynthetic pathway towards neutral lipid accumulation especially triacylglycerol (TAG), the most concentrated form of metabolic energy in eukaryotic cells comprised of three fatty acids esterified with a glycerol backbone (Fan et al. 2011). While nitrogen limitation is the most common growth condition used to increase intracellular lipid accumulation (Illman et al. 2000; Stephenson et al. 2010; Sharma et al. 2012), availability of the other microelements, i.e., cadmium (Chia et al. 2013), sulfur (Cakmak et al. 2012), and iron (Liu et al. 2008), has also been shown to cause significant changes in the lipid biosynthesis in algae (Lari et al. 2016).

Exploitation of microalgal strains with high biomass productivity and lipid accumulating capacity is a major challenge for commercialization of biodiesel (Singh et al. 2014). Among various green microalgae, *Tetradesmus obliquus* (previously known as *Scenedesmus obliquus* and *Acutodesmus obliquus*) is one of the most intensively studied species with favorable features like rapid growth rate, efficient CO_2 fixation, high lipid productivity, and appropriate fatty acid profile including oleic, palmitic, and stearic acids which makes it a highly exceptional candidate for renewable biodiesel production (Gris et al. 2014; Wu and Miao 2014; Álvarez-Díaz et al. 2015; Abomohra et al. 2018). It has also been shown that iron is an essential micronutrient in all photosynthetic organisms and functions as a cofactor in the transfer of electrons from photosystem II to photosystem I (Concas et al. 2014). Moreover, the redox properties of iron are necessary for numerous metabolic processes such as nitrogen assimilation, cellular respiration, carbon fixation, and glycerolipid biosynthesis (Urzica et al. 2013; Che et al. 2015; Marchetti and Maldonado 2016). To date, the effect of iron on algae has principally focused on some algal species like *Chlamydomonas reinhardtii* (Terauchi et al. 2010), *Chlorella vulgaris* (Wan et al. 2014), and *Neochloris oleoabundans* (Sun et al. 2014), while other species have

not been extensively investigated. Accordingly, the present study was conducted to assess the effect of iron on the growth, lipid content, and fatty acid profile of *T. obliquus* under laboratory conditions. The key parameters for determining biodiesel quality were also evaluated based on the fatty acid profile.

Materials and methods

Culture collection

Tetradesmus obliquus was isolated from a fresh water body of Darakeh village, Shemiranat County, Iran, and purified based on the procedure suggested by Stanier et al. (1971) by plate streaking on 1.2% agar BG11 medium at pH 7.0. The process was repeated in the medium containing antibiotics such as ampicillin (100 ppm), cefotaxime (100 ppm) and erythromycin (20 ppm) to obtain an axenic culture of this strain. The isolated cells were cultivated at 25 °C in 1-L Erlenmeyer flasks with 500 mL autoclaved medium. The flasks were placed under aseptic condition in a growth chamber, illuminated by cool white fluorescent lamps under a photon flux of 120 μmol photon m^{-2} s^{-1} with a photoperiod of 16:8 h (light/dark), and continuously shaken at a rate of 110 rpm. The media were aerated using mixed gases (4% CO_2, v/v) at a flow rate of 1800 L h^{-1}, while the solution pH was kept at 7.0 ± 0.2 by bubbling the flue gas.

Microscopic evaluation and species identification

Initial identification of the isolated strain was carried out on the basis of morphological characteristics under a compound microscope at × 1000 magnification. The identity of the isolate was further confirmed by 18S rDNA gene sequence analyses. The genomic DNA was extracted from the algal strain (5 mg dry mass) by CTAB method (Doyle and Doyle 1987). The 18S rDNA primers NS1–5′-GTAGTCATATGCTT GTCTC-3′ and NS6–5′-GCATCACAGACCTGTTATTG CCTC-3′ were used for amplification of the genomic DNA. PCR amplification was performed in a reaction mixture containing 100 mM dNTP, 0.5 mM of each primer, 25 ng template DNA, and 10× Taq buffer, 1.25 U of Taq polymerase (Sinacolon, Tehran). DNA was amplified on a MyCycler gradient DNA amplifier (Bio-Rad, USA) based on the following amplification profile: 95 °C for 1 min initial denaturation, followed by 35 cycles of 95 °C for 30 s, primer annealing for 30 s, and extension for 30 s at 72 °C. Sequences of 18S rDNA gene were determined by the ABI PRISM 3100 DNA Sequencer (Applied Biosystems, USA) and compared with other publically available sequences in GenBank using the basic local alignment search tool (BLAST) algorithm to identify homologous taxa available on the National Center for

Biotechnology Information (NCBI) database (Altschul et al. 1990). Phylogenetic tree was drawn based on the neighbor-joining algorithm using molecular evolutionary genetics analysis (MEGA) 6.0 software (Tamura et al. 2013).

Experimental design for iron supplementation

Axenic *T. obliquus* was grown in BG11 medium without iron addition for 6 days to attain the required cell density for any given experiment. In order to investigate the effect of iron on growth and lipid properties of *T. obliquus*, five types of modified BG11 medium were prepared by adding 10^{-4}, 10^{-3}, 10^{-2}, and 10^{-1} mmol L^{-1} iron in the ferric form ($FeCl_3 \cdot 6H_2O$/EDTA) to the iron-absent BG11 medium as control. The $FeCl_3 \cdot 6H_2O$/EDTA was prepared by dissolving 1 g Na_2EDTA and 81 mg $FeCl_3 \cdot 6H_2O$ in 50 mL distilled water and HCl (0.1 N), respectively. The solutions were then mixed to prepare 3 mmol $FeCl_3 \cdot 6H_2O$/EDTA.

At the beginning of the experiment, the algal cells were harvested from the stock culture by centrifugation at $3578 \times g$ for 15 min. The algae were washed twice with double distilled water and resuspended at an initial inoculation density of 2×10^6 cells mL^{-1} in 1-L Erlenmeyer flasks containing the corresponding experimental medium (BG11 medium without iron supplementation or one of the nutrient-modified media). The cultures were then incubated for 20 days under the same temperature, irradiance, aeration, and photoperiod as described above. All of the experiments were carried out in quadruplicate.

Growth and biomass determination

The cell density of each culture was determined at regular intervals (twice a day) by counting using a hemocytometer (improved Neubauer) under an inverted biological phase contrast microscope. The specific growth rate was determined based on the following equation: $\mu = (\ln N_2 - \ln N_1)/(t_2 - t_1)$, where μ is the specific growth rate (day^{-1}), N_1 is the initial cell density (t_1), and N_2 is the cell density at the end of logarithmic growth phase (t_2) (Xu and Boeing 2014). For dry weight determination, biomass was separated from the medium by filtering 20 mL of the culture through a pre-weighted glass fiber paper filter (Whatman GF/C) and drying at 105 °C for 12 h to constant weight. The algal dry weight was measured by subtracting the dry weight of loaded membrane from the respective blank filter. The biomass productivity was calculated according to the following equation: $BP = (DW_2 - DW_1)/(t_2 - t_1)$, where BP was the biomass productivity ($g L^{-1} day^{-1}$), DW_2 was the algal dry weight at the end of logarithmic growth phase (t_2), and DW_1 was the algal dry weight at the beginning of the cultivation period (t_1) (Rai and Gupta 2016).

Lipid extraction and nutrient analysis

Once the culture reached the stationary phase, lipid content of algae in each replicate was gravimetrically determined. Microalgae were harvested by centrifuging at $12000 \times g$ for 15 min using a high-speed centrifuge (3-30K, SIGMA Laborzentrifugen GmbH, Germany). The resulting pellets were then washed twice with distilled water and freeze-dried at − 46 °C. The total lipid extraction was done according to the Bligh and Dyer (1959) method modified by Huang et al. (2014). In brief, 0.2 g of freeze-dried pellets was extracted with a mixture of chloroform:methanol (2:1, *v:v*) for 24 h and subjected to ultrasonication (70 Hz at ambient temperature twice for 30 min) during the extraction for breaking the algal cells. The suspension was then filtered to remove biomass residues and the filtrate was washed twice with KCl solution. The lower liquid was transferred to a pre-weighed tube and the solvent was evaporated to dryness at − 90 °C using a vacuum freeze dryer. The lipid content was measured gravimetrically and shown as the percentage of lipid weight in the cell dry weight.

The NO_3-N and PO_3-P concentrations in culture media were spectrophotometrically evaluated using a water quality autoanalyzer (DR-6000, Hach, USA) according to the respective standard methods (APHA 1998). Before analyzing, the medium samples were filtered through a 0.45-μm-pore-size syringe filter (Sartorius, Germany) to remove algal cells and any other trace of possible interference from suspended particles in the culture medium.

Lipid characterization

Fatty acid profile

The extracted lipid was subjected to saponification with ethanolic KOH (20%, *w/v*) at ambient temperature over the night. The solution was acidified with 5 N·HCl before extraction with petroleum ether at 40–60 °C to liberate fatty acids from their potassium salts. The organic phase containing fatty acid methyl esters (FAMEs) was collected for further analysis. The lipid components were analytically verified by gas chromatography using the method described by Huang et al. (2014). In brief, the FAMEs were detected after injecting the sample into a gas chromatograph spectrometer (Hewlett-Packard 5890 series II, USA) equipped with Omegawax 320 column (30 m × 0.32 mm I.D. × 0.25 μm; Supelco, USA) and a flame-ionization detector (FID). Column injector and detector temperature were held at 260 °C. The oven temperature was programmed to rise from 60 to 170 °C at a rate of 10 °C min^{-1}, followed by an increase to 180 °C at a rate of 2 °C min^{-1}, where it was maintained constant for 2 min. The temperature was then increased to 230 °C at a rate of 2 °C min^{-1}, kept hold for 1 min, thereafter increased to

240 °C at a rate of 1 °C min^{-1}, where it remained unchanged until all FAMEs were eluted. Helium was used as carrier gas at a flow velocity of 30 mL min^{-1}. The peaks were identified by comparison of retention time with those in authentic standards (Supelco 37 Components FAME Mixture, USA). The fatty acid content was determined on a weight percentage basis by measuring the area under the peak corresponding to the respective fatty acid.

Biodiesel quality assessment

The biodiesel properties of extracted lipid were determined by assessing the saponification value (SV), iodine value (IV), and cetane number (CN) based on the fatty acid profile. The values were assessed by empirical formulas mentioned in Eqs. (1–3) (Osundeko et al. 2013):

$$SV = \sum (560 \times F)/MW \qquad (1)$$

$$IV = \sum (254 \times F \times D)/MW \qquad (2)$$

$$CN = (46.3 + 5458/SV) - (0.225 \times IV) \qquad (3)$$

where F is the percentage of each fatty acid, MW is the molecular mass of respective fatty acid, and D is the number of its double bonds.

Statistical analysis

Results are presented as means of four replicates ± standard deviation (SD). Significant differences between means were determined using one-way analysis of variance (ANOVA) at probability level $p < 0.05$. When the F value showed significant difference among treatments, multiple comparisons among the means were performed using Duncan's new multiple range test. All statistical analysis was carried out using the software SPSS 12.0 statistical package for Windows (SPSS Inc.).

Results

Morphological features and molecular characterization of *T. obliquus*

Microscopic observation showed that the isolated strain was oval in shape with distinct polar conoidal protuberances of the cell wall. The cells were single or joined along the longer axe to form four- or (less frequently) eight-celled coenobia characterized as typical morphological features of genus *Tetradesmus*. Further characterization up to the species level was done based on the phylogenetic analysis, where the 18S rDNA gene sequence of the isolate showed 99% identity to

Tetradesmus obliquus (accession number: MG969897.1) annotated and deposited to NCBI GenBank (Fig. 1).

Effect of ferric iron concentration on growth rate and nutrient assimilation of *T. obliquus*

The growth rates of algae grown in media supplemented with 10^{-4}, 10^{-3}, and 10^{-2} mmol L^{-1} ferric iron concentrations were higher than those grown in the medium without iron supplementation (Fig. 2). However, the algae treated with 10^{-1} mmol L^{-1} ferric iron had the lowest cell densities after 4 days compared with those treated with lower iron concentration. From the 6th day of the experiment, the culture supplemented with 10^{-2} mmol L^{-1} ferric iron exhibited the highest growth rate and retained this pattern until the end of the experiment. The algae grown in control medium reached stationary phase after 10 days, while algae cultured in medium supplemented with equal to or lower than 10^{-2} mmol L^{-1} ferric iron remained in the exponential growth phase over the next 6 days.

The assimilation of nitrogen (NO$_3$-N) and phosphorus (PO$_3$-P) by *T. obliquus* in the media is shown in Fig. 3. The concentration of NO$_3$-N decreased from 314.87 ± 4.15 to 267.54 ± 2.94 mg L^{-1} in medium without iron supplementation after 6 days and remained significantly unchanged thereafter ($p < 0.05$). The lowest NO$_3$-N concentration was obtained in the medium supplemented with 10^{-2} mmol L^{-1} ferric iron at the end of the experiment. A similar trend was observed for the assimilation of phosphorus (PO$_3$-P) by the *T. obliquus* with the lowest concentration in the culture supplemented with 10^{-2} mmol L^{-1} ferric iron at the end of the experiment.

The specific growth rate of microalgae was significantly affected by ferric iron supplementation (Fig. 4). The highest specific growth rate, 0.36 ± 0.04 day^{-1}, of *T. obliquus* was achieved in the growth medium supplemented with 10^{-2} mmol L^{-1} ferric iron concentration, while higher and lower iron supplementations resulted in significantly lower specific growth rates ($p < 0.05$). However, there was no significant difference in the specific growth rate of algae grown in medium supplemented with 10^{-1} mmol L^{-1} ferric iron and non-supplemented medium.

Effect of ferric iron concentration on lipid accumulation and biomass productivity of *T. obliquus*

The ferric iron concentration significantly affected the lipid content of *T. obliquus* after reaching the stationary phase (Table 1). Algae grown in the iron-absent BG11 medium exhibited a lipid content of $15.37 \pm 0.62\%$ DW. By increasing the ferric iron concentration in the growth medium, the lipid content increased and reached a maximum of $34.19 \pm 1.93\%$ DW in medium supplemented with 10^{-1} mmol L^{-1} ferric iron. On the other hand, the biomass productivity was enhanced

Fig 1 16S rDNA-based phylogenic identification tree of isolated strain drawn by multiple sequence alignment with neighbor-joining method using the MEGA 6.0 software. The BLAST result has shown that the isolated strain is most closely related (99% identity) to *Tetradesmus obliquus* (GenBank accession number: MG969897.1)
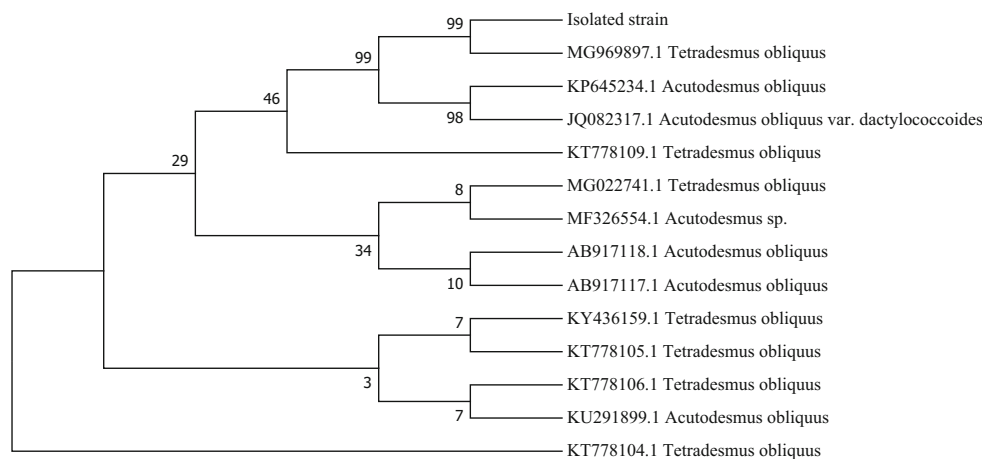
significantly with increasing iron concentration from 251.47 ± 1.29 mg L^{-1} day^{-1} in medium supplemented with 10^{-1} mmol L^{-1} ferric iron concentration to 459.20 ± 2.37 mg L^{-1} day^{-1} in medium supplemented with 10^{-2} mmol L^{-1} ferric iron concentration ($p < 0.05$), demonstrating that culture conditions required to maximize the lipid content do not comply with those for maximizing the algal growth.

Effect of ferric iron concentration on fatty acid profile of *T. obliquus*

The lipid produced from *T. obliquus* in all media contains a fatty acid profile of mainly saturated fatty acids (SFA; 32.36 ± 2.27 to $54.8 \pm 2.76\%$) and monounsaturated fatty acids (MUFA; 22.75 ± 1.08 to $42.3 \pm 2.60\%$) (Table 2). Although the major fatty acid compositions were similar in algae grown in control medium and those grown in media supplemented with ferric iron, there were considerable differences in their

percentage composition. Palmitic acid (C16:0; $27.85 \pm 0.93\%$), oleic acid (C18:1; $31.48 \pm 2.17\%$), alpha-linolenic acid (C18:3; $18.42 \pm 2.08\%$), palmitoleic acid (C16:1; 9.28 ± 0.54), and linoleic acid (C18:2; $6.29 \pm 0.57\%$) are the most abundant fatty acids found in *T. obliquus* grown in the medium without iron supplementation. In spite of no significant difference in the percentage composition of lauric acid (C12:0) and linoleic acid among the experimental treatments, percentage composition of myristic acid (C14:0), pentadecanoic acid (C15:0), palmitic acid, margaric acid (C17:0), and stearic acid (C18:0), arachidic acid (C20:0), and behenic acid (C22:0) of *T. obliquus* increased significantly by increasing the ferric ion concentration in the growth medium ($p < 0.05$). On the other hand, percentage composition of palmitoleic acid, oleic acid, alpha-linolenic acid, and paullinic acid (C20:1) significantly decreased by increasing the ferric iron supplementation in the growth medium ($p < 0.05$). As the ferric iron supplementation in the culture medium increased from 10^{-2} to 10^{-1} mmol L^{-1}, percentage

Fig. 2 Growth curve of *Tetradesmus obliquus* cultured under different ferric iron concentrations (mmol L^{-1}). Error bars represent ± SD of four replicates
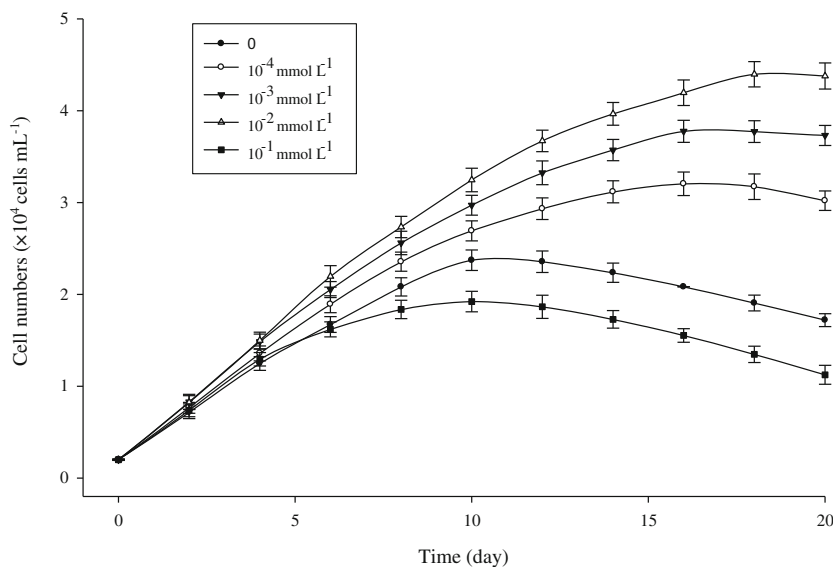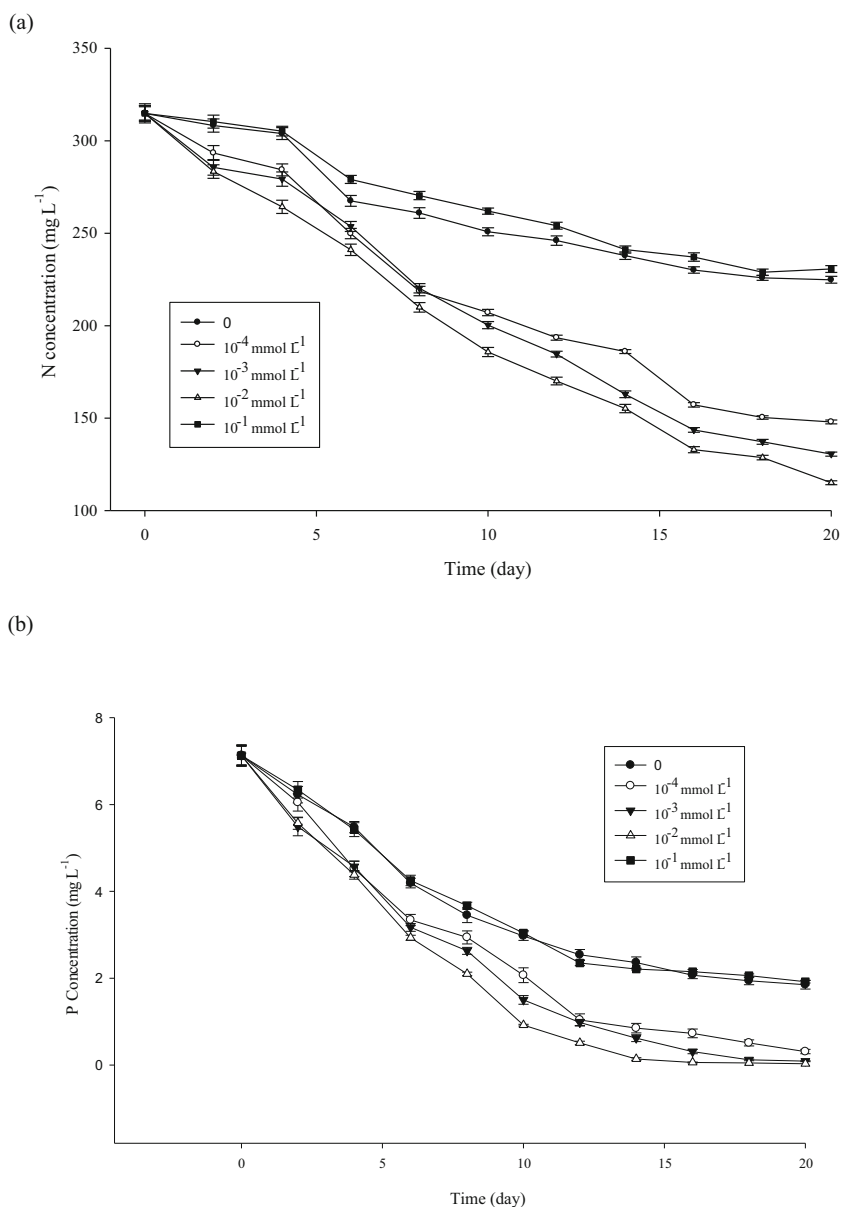
Fig. 3 Profile of nitrogen (**a**) and phosphorous (**b**) assimilation by *Tetradesmus obliquus* cultured under different ferric iron concentrations (mmol L^{-1}). Error bars represent ± SD of four replicates

composition of myristic acid, palmitic acid, margaric acid, arachidic acid, and behenic acid increased significantly, whereas the percentage compositions of palmitoleic acid and oleic acid were significantly decreased ($p < 0.05$). There is also a significant trend in SFAs by increasing the ferric iron supplementation in the growth medium, while MUFAs and PUFAs significantly decreased ($p < 0.05$).

Effect of ferric iron concentration on the properties of biodiesel from *T. obliquus*

The key parameters of biodiesel quality of *T. obliquus* grown in media with different iron supplementations were calculated based on the fatty acid profile and are presented in Table 3. The CN values showed the increasing trend with incremental

ferric iron supplementation and reached to the highest value of 64.69 in the culture with 10^{-2} mmol L^{-1} ferric iron. Conversely, the IV significantly decreased by increasing the ferric iron concentration to the least of 37.30 g I$_2$ 100 g^{-1} in medium supplemented with 10^{-1} mmol L^{-1} ferric iron ($p < 0.05$), although no significant difference was found between media supplemented with 10^{-2} and 10^{-1} mmol L^{-1} ferric iron. There was also no significant difference in SV of oil extracted from algae grown under different iron concentrations.

Discussion

Because of high biomass productivity, short generation time, and high lipid accumulation, microalgae are currently
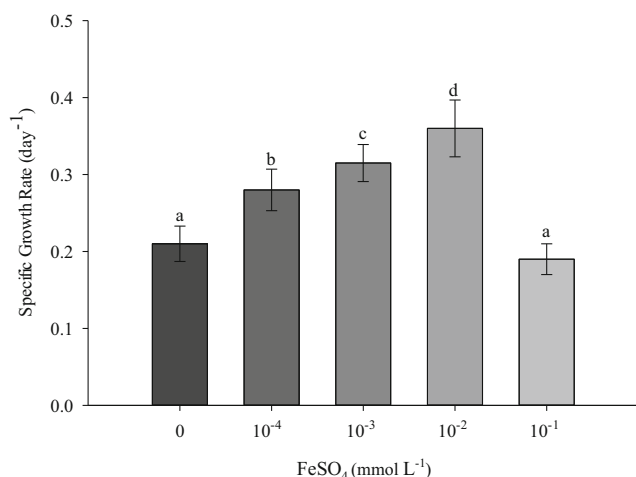
Fig. 4 Specific growth rate of *Tetradesmus obliquus* cultured under different ferric iron concentrations (mmol L^{-1}). Different small letters on each column indicate significant difference ($p < 0.05$). Error bars represent ± SD of four replicates

considered an alternative feedstock for biodiesel production (Schenk et al. 2008; Demirbas 2011). However, production of microalgae not only requires important inorganic macronutrients in the forms of nitrogen and phosphorus but also depends on appropriate supplementation of micronutrients like zinc, iron, copper, manganese, and cobalt that influence cell growth (Sunda et al. 2005; Brennan and Owende 2010). Iron is an essential trace element necessary for major cellular functions that require electron transfer reactions including photosynthesis, respiration, and nitrogen assimilation (Che et al. 2015; Marchetti and Maldonado 2016). It plays an important role in biosynthesis of δ-aminolevulinic acid, the first compound in the porphyrin synthesis pathway leading to chloroplast formation (Miller et al. 1995). Iron also forms a prosthetic group of several metallo-enzymes involved in oxygen consumption rate and nitrate-reducing systems (Glass et al. 2009; Yeesang and Cheirsilp 2011; Dlouhy and Outten 2013). In the present study, the best growth of *T. obliquus* was obtained in medium supplemented with 10^{-2} mmol L^{-1} ferric iron, while further Fe supplementation resulted in a significant decrease of growth rate. This confirms the hypothesis that proper supplementation of ferric iron is necessary to optimize the growth performance, while high concentrations would inhibit the algal growth. Iron

deficiency restricts the light harvesting, electron transfer, and energy conversion process, which can cause a considerable enhancement in the biomass of microalgae (Terauchi et al. 2010). On the other hand, excessive iron concentrations can produce hydroxyl radicals through Fenton or Haber-Weiss reactions, leading to oxidative stress in the cell membranes via lipid peroxidation or oxidation of thiol groups in proteins and DNA (Keenan et al. 2009; Kadar et al. 2011).

Algal species can increase their specific growth rate when exposed to an active form of iron concentration. Wan et al. (2014) found that *Chlorella sorokiniana* shows the fastest growth rates under optimal iron concentration of 10^{-2} mmol L^{-1}, reaching 2.1-fold of that without iron supplementation in the culture medium. A dramatic rise in the growth rate of *Phaeodactylum tricornutum* was also obtained as the iron concentration increased to 1.2×10^{-4} mol L^{-1} iron in the growth medium after an 8-day starvation for exhaustion of cellular iron reserves (Zhao et al. 2018). Ruangsomboon et al. (2013) found the highest specific growth rate of *Scenedesmus dimorphus* by cultivation with an initial iron concentration (FeSO$_4$) of 36 mg L^{-1}. Iron supplementation of up to 10^{-2} mmol L^{-1} caused the highest growth rate of *T. obliquus* in the current study; meanwhile, lower and higher iron concentrations resulted in lower growth rates. This implies that the appropriate iron concentration for maximizing algal growth is a unique characteristic related to the biological demands of each species.

High lipid productivity is one of the main characteristics to select a certain microalga for feasible biodiesel production (Griffiths and Harrison 2009; Abomohra et al. 2016). During unfavorable conditions, many microalgae change their metabolic pathways to accumulate more lipid content, which are high in energy and similar to conventional fuels (Li et al. 2011). There are many studies that have focused on the lipid accumulation of microalgae by iron manipulation in the culture medium. Sun et al. (2014) found that Fe^{3+} concentration of 0.037 mmol L^{-1} induces the highest triacylglyceride productivity of 51.58 mg L^{-1} day^{-1} in *Neochloris oleoabundans*, while further supplementation did not enhance the lipid content. Lipid accumulation in four strains of *Botryococcus* was also improved by supplementing a high level of iron and light intensity under nitrogen deficiency (Yeesang and Cheirsilp

Table 1 Lipid content and biomass productivity of *Tetradesmus obliquus* cultured under different iron concentrations after reaching the stationary phase

Ferric iron concentration (mmol L^{1})	Lipid content (% DW)	Biomass productivity (mg L^{-1} day^{-1})
0	15.37 ± 0.62a	261.75 ± 1.54a
10^{-4}	24.75 ± 1.19b	342.95 ± 1.89b
10^{-3}	28.36 ± 1.45c	379.71 ± 1.93b
10^{-2}	30.27 ± 1.80d	459.20 ± 2.37c
10^{-1}	34.19 ± 1.93e	251.47 ± 1.29a

Different small letters on each column indicate significant difference ($p < 0.05$). Values are presented as means ± standard deviations of four replicates

Table 2 Fatty acid methyl esters (FAME) profile of *Tetradesmus obliquus* cultured under different iron concentrations after reaching the stationary phase

	Ferric iron concentration (mmol L^1)				
	0	10^{-4}	10^{-3}	10^{-2}	10^{-1}
C12:0 (lauric acid)	0.74 ± 0.09	0.79 ± 0.08	0.82 ± 0.06	0.83 ± 0.04	0.86 ± 0.05
C14:0 (myristic acid)	0.31 ± 0.03a	0.44 ± 0.06a	0.56 ± 0.04ab	0.76 ± 0.02b	1.05 ± 0.09c
C15:0 (pentadecanoic acid)	1.12 ± 0.24a	1.13 ± 0.19a	1.24 ± 0.14a	2.13 ± 0.25b	2.72 ± 0.95b
C16:0 (palmitic acid)	27.85 ± 0.93a	30.57 ± 0.84b	32.94 ± 1.03c	34.71 ± 1.09c	36.59 ± 1.07d
C16:1 (palmitoleic acid)	9.28 ± 0.54d	7.39 ± 0.45c	5.21 ± 0.37b	3.94 ± 0.29b	1.03 ± 0.11a
C16:2 (7,10-hexadecanoic acid)	0.58 ± 0.04b	0.36 ± 0.02b	0.22 ± 0.01ab	0.18 ± 0.01a	0.07 ± 0.01a
C17:0 (margaric acid)	0.24 ± 0.01a	1.39 ± 0.10b	2.87 ± 0.14b	4.58 ± 0.19c	5.78 ± 0.22d
C18:0 (stearic acid)	1.73 ± 0.28a	2.84 ± 0.15b	2.91 ± 0.019b	3.08 ± 0.17b	3.29 ± 0.18b
C18:1 (oleic acid)	31.48 ± 2.17d	28.37 ± 1.97c	26.15 ± 1.85b	24.59 ± 1.62b	20.83 ± 1.27a
C18:2 (linoleic acid)	6.29 ± 0.57	6.04 ± 0.47	5.92 ± 0.39	5.47 ± 0.38	5.32 ± 0.29
C18:3 (alpha-linolenic acid)	18.42 ± 2.08c	17.24 ± 1.36bc	16.35 ± 1.29b	14.59 ± 1.08ab	13.17 ± 0.85a
C20:0 (arachidic acid)	0.37 ± 0.02a	1.54 ± 0.12b	2.86 ± 0.37c	3.05 ± 0.29d	4.51 ± 0.34e
C20:1 (paullinic acid)	1.54 ± 0.14b	1.27 ± 0.17b	1.03 ± 0.06a	0.92 ± 0.08a	0.89 ± 0.08a
C22:00 (behenic acid)	0.05 ± 0.01a	0.63 ± 0.02b	0.92 ± 0.07c	1.2 ± 0.08c	3.91 ± 0.23d
∑SFAs	32.36 ± 2.27a	38.77 ± 2.39b	44.13 ± 2.45c	49.11 ± 2.61d	54.8 ± 2.76e
∑MUFAs	42.30 ± 2.60e	37.03 ± 2.37d	32.39 ± 1.69c	29.45 ± 1.25b	22.75 ± 1.08a
∑PUFAs	25.29 ± 1.78e	23.64 ± 1.69d	22.49 ± 1.58c	20.24 ± 1.37b	18.54 ± 1.27a

SFA saturated fatty acids, *MUFA* monounsaturated fatty acids, *PUFA* polyunsaturated fatty acids. Different small letters on each raw indicate significant difference ($p < 0.05$). Values are presented as means ± standard deviations of four replicates

2011). Likewise, a greater lipid content was found in the marine strain *Chlorella vulgaris*, when cells are cultured in a medium containing 0.012 mol L^{-1} FeCl$_3$ compared with those cultured in the medium with lower iron concentrations (Liu et al. 2008). Findings of the current study illustrated that the lipid content of *T. obliquus* accumulated from 15.37 ± 0.62 to 34.19 ± 1.93% DW by increasing the medium iron concentration to 10^{-1} mol L^{-1} ferric iron, indicating that some biosynthetic mechanisms associated with the lipid accumulation were probably altered by high iron concentrations (Sun et al. 2014). The chloroplast and mitochondrion are two cell organelles with many iron-dependent proteins which their functions are necessary in the electron transfer pathways (Glaesener et al. 2013). In photosynthetic organisms, NADPH is produced by ferredoxin-NADP$^+$ reductase and used as a reducing agent for anaerobic reactions such as lipid accumulation

(Doubnerová and Ryšlavá 2011). Furthermore, iron deprivation can increase the gene expression of diacylglycerol acyl-transferase which is one of the important enzymes related to the lipid metabolic process (Hernández-Torres et al. 2016), catalyzing the synthesis of triglycerides from diacylglycerol and Acyl-CoA (Goncalves et al. 2016).

The appropriate condition to maximize lipid production in algal species usually does not match with those leading to the best biomass production. Similarly, Che et al. (2015) reported that 150 μM Fe augmentation in BG11 medium results in the highest dry cell weight of *Monoraphidium* sp., whereas the maximum lipid productivity was obtained at 50 μM Fe inoculation. A comparable phenomenon has been observed in the present study which may ultimately lead to a two-step process for lipid production from *T. obliquus*, in which biomass should be separated from the culture supplemented with

Table 3 The biodiesel properties of *Tetradesmus obliquus* cultured under different iron concentrations after reaching to the stationary phase

Ferric iron concentration (mmol L^1)	CN	IV (g I$_2$ (100 g)$^{-1}$)	SV (mg KOH g^{-1})
0	49.61a	102.68c	206.67
10^{-4}	61.61b	53.64b	199.35
10^{-3}	63.37b	47.22b	197.08
10^{-2}	64.69b	39.53a	200.04
10^{-1}	64.34b	37.30a	206.51

CN cetane number, *IV* iodine value, *SV* saponification value. Different small letters on each column indicate significant difference ($p < 0.05$)

10^{-2} mmol L^{-1} ferric iron concentration to achieve the maximum algal biomass in the first step and then inoculated to the culture supplemented with 10^{-1} mmol L^{-1} ferric iron concentration to reach the highest lipid productivity in the second step, leading to optimization of lipid production from *T. obliquus*. However, a two-step strategy of algal cultivation may lead to more manpower and energy consumption and thus increase the cost of biofuel production from microalgae especially at the large-scale implementation (Sun et al. 2014).

Biodiesel is chemically defined as the monoalkyl esters of long chain fatty acids derived from renewable lipid feedstock via a transesterification process (Ashokkumar et al. 2015). From an economic point of view, fatty acid composition influences the biodiesel properties such as viscosity, cetane number, flash point, and oxidation stability (Islam et al. 2013). It has been shown that fatty acid with long carbon chain (C16–18) is more preferable for biodiesel fuel (Ruangsomboon et al. 2013). Lipid of *T. obliquus* is principally composed of saturated fatty acids and monounsaturated fatty acids (Shao et al. 2017), which shows its suitability for biodiesel production. However, the present findings illustrated that *T. obliquus* grown in medium containing 10^{-1} mmol L^{-1} ferric iron had significantly higher myristic acid, palmitic acid, margaric acid, arachidic acid, and behenic acid compared with those cultured at lower iron concentrations ($p < 0.05$), indicating that iron supplementation could improve the quality of lipid obtained from *T. obliquus* as a feedstock for biodiesel production. On the other hand, percentage composition of palmitoleic acid, 7,10-hexadecanoic acid, oleic acid, alpha-linolenic acid, and paullinic acid in *T. obliquus* oil declined by increasing iron concentration in the growth medium which could be explicated by oxidative damages of unsaturated fatty acids induced by high iron concentrations via Fenton-type reactions (Ayala et al. 2014).

As the ferric ion concentration increased, the total amount of SFAs obtained from *T. obliquus* in the present study significantly enhanced, while the amount of MUFAs and PUFAs declined ($p < 0.05$). This phenomenon may be explained by creating reactive oxygen species (ROS) in the presence of excess iron concentration via Fenton-type reactions (Wu et al. 2010). Iron is an essential micronutrient required in biological redox systems of all aerobic organisms (Søndergaard 2009; Li-Beisson et al. 2019). However, such redox activity can generate various ROS by the Haber-Weiss reaction which in turn may attack lipids containing carbon–carbon double bonds, especially PUFAs as major substrates for lipid peroxidation (Kehrer 2000; Ayala et al. 2014). The fatty acid profile changes of *T. obliquus* in the present study were generally consistent with those reported for *Tetraselmis subcordiformis*, *Nannochloropsis oculata*, and *Pavlova viridis* (Huang et al. 2014). However, Urzica et al. (2013) stated that iron starvation leads to formation of more SFAs and lower PUFAs in *C. reinhardtii*. The increase of PUFAs was also noticed by Pádrová et al. (2015) who investigated the relationship

between intracellular lipid production and nanoscaled zero-valent iron concentration in *Desmodesmus subspicatus*. These contradictory results may imply that response of fatty acid biosynthesis in microalgae to high ferric iron concentrations is a species-specific feature.

Based on the European standard EN14214, the percentage of linolenic acid and polyunsaturated fatty acids with equal to or more than four double bonds should not increase from 12% and from 1%, respectively (Chisti 2007; Gouveia and Oliveira 2009). In the current research, the linolenic acid showed no significant difference in medium supplemented with different ferric iron supplementations. No polyunsaturated fatty acid with more than three bonds was also detected in the fatty acid profile of *T. obliquus* cultured in all treatments.

The cetane number (CN) is one of the important biodiesel properties related to the ignition delay as the time between the start of injection and the first identifiable pressure increases during combustion. The CN increases with the length of the unbranched carbon chain of the FAME components, resulting in better combustion and lower nitrous oxide emission, followed by the less occurrence of engine knocking (Knothe 2012; Arias-Peñarands et al. 2013). According to the US standards (ASTM D6751) and European standards (EN14214) for biodiesel, the minimum CN should be 47.0 and 51.0, respectively. As shown in Table 3, the estimated CN for *T. obliquus* grown under different iron supplementations meets the minimum values of the mentioned standards for biodiesel production and improves by increasing the medium iron concentration.

Microalgal biodiesel is also evaluated by the iodine value (IV), a prime indicator for determining the degree of unsaturation in fatty acids. The higher IV number (iodine in gram consumed by 100 g of a sample) denotes the higher possibility of oxidation, deposit formation, and deterioration of the biodiesel lubricity (Nascimento et al. 2013). Under different iron concentrations, the iodine value of the extracted lipid from *T. obliquus* was recorded in the range of 37.30 to 102.68 g I_2 $(100\ g)^{-1}$ oil which meets the biodiesel quality criterion of less than 120 g I_2 $(100\ g)^{-1}$ oil prescribed by the European standards (EN14214) for biodiesel production.

The saponification value (SV) is another biodiesel property expressed by potassium hydroxide in milligram for the complete saponification of 1 g of oil. Although the European standard has not included the SV as the restricted property of biodiesel oil (Predojević et al. 2012), the SVs of *T. obliquus* under different iron supplementations in the current research were all under 206.67 mg KOH g^{-1} which were around those reported for the other potential feedstock microalgal strains for biodiesel production like *Chlorella luteoviridis* (207.91 mg KOH g^{-1}; Osundeko et al. 2013), *Chlamydomonas* sp. (206.87 mg KOH g^{-1}; Sivaramakrishnan and Incharoensakdi 2017), *Scenedesmus abundans* (205.08 mg KOH g^{-1}; Rai and Gupta 2016), *Chlorella sorokiniana* (104 mg KOH g^{-1}; Qiu et al. 2017), and *Tolypothrix tenuis* (206.22 mg KOH g^{-1};

Anahas and Muralitharan 2018). However, this parameter is highly variable and directly related to the technology used for biodiesel production (Nascimento et al. 2013).

In conclusion, the findings of the present study illustrated that iron concentration had a strong influence on the growth rate, lipid accumulation, and fatty acid composition of *T. obliquus*. The peak of the growth rate (0.36 ± 0.03 day^{-1}) and lipid content ($34.19 \pm 1.93\%$ DW) of the microalga was obtained in the media supplemented with 10^{-2} and 10^{-1} mmol L^{-1} ferric iron supplementations, respectively. The highest proportion of the saturated fatty acids and the lowest proportion of unsaturated fatty acids were also achieved by adding 10^{-1} mmol L^{-1} ferric iron to the growth medium. Quality of biodiesel produced from *T. obliquus* met the specification of the European biodiesel standard (EN14214) in all experimental media, and ferric iron supplementation could be used to optimize the lipid characteristics of *T. obliquus* for biodiesel production.

References

Abomohra AE, Jin W, El-Sheekh M (2016) Enhancement of lipid extraction for improved biodiesel recovery from the biodiesel promising microalga Scenedesmus obliquus. Energy Convers Manag 108:23–39

Abomohra AE, Jin W, Sagar V, Ismail GA (2018) Optimization of chemical flocculation of Scenedesmus obliquus grown on municipal wastewater for improved biodiesel recovery. Renew Energy 115:880–886

Ahmad AL, Yasin NH, Derek CJC, Lim JK (2011) Microalgae as a sustainable energy source for biodiesel production: a review. Renew Sust Energ Rev 15:584–593

Altschul SF, Gish W, Miller W, Myers EW, Lipman DJ (1990) Basic local alignment search tool. J Mol Biol 215:403–410

Álvarez-Díaz PD, Ruiz J, Arbib Z, Barragán J, Garrido-Pérez MC, Perales JA (2015) Wastewater treatment and biodiesel production by Scenedesmus obliquus in a two-stage cultivation process. Bioresour Technol 181:90–96

Amaro HM, Guedes AC, Malcata FX (2011) Advances and perspectives in using microalgae to produce biodiesel. Appl Energy 88:3402–3410

Anahas AMP, Muralitharan G (2018) Characterization of heterocystous cyanobacterial strains for biodiesel production based on fatty acid content analysis and hydrocarbon production. Energy Convers Manag 157:423–437

APHA (1998) Standard methods for examination of water and wastewater, twentieth ed. American Public Health Association, Washington, DC

Arias-Peñaranda MT, Cristiani-Urbina E, Montes-Horcasitas CM, Esparza-Garćia F, Torzillo G, Cañizares-Villanueva RO (2013) Scenedesmus incrassatulus CLHE-Si01: A potential source of renewable lipid for high quality biodiesel production. Bioresour Technol 140:158–164

Ashokkumar V, Salam Z, Tiwari ON, Chinnasamy S, Mohammed S, Ani FN (2015) An integrated approach for biodiesel and bioethanol production from Scenedesmus bijugatus cultivated in a vertical tubular photobioreactor. Energy Convers Manag 101:778–786

Ayala A, Muñoz MF, Argüelles S (2014) Lipid peroxidation: production, metabolism, and signaling mechanisms of malondialdehyde and 4-hydroxy-2-nonenal. Oxidative Med Cell Longev 2014:1–31

Bligh EG, Dyer WJ (1959) A rapid method of total lipid extraction and purification. Can J Physiol Pharm 37:911–917

Borowitzka MA (1992) Algal biotechnology products and processes - matching science and economics. J Appl Phycol 4:267–279

Borowitzka MA, Moheimani NR (2013) Sustainable biofuels from algae. Mitig Adapt Strateg Glob Chang 18:13–25

Brennan L, Owende P (2010) Biofuels from microalgae—a review of technologies for production, processing, and extractions of biofuels and coproducts. Renew Sust Energ Rev 14:557–577

Cakmak T, Angun P, Demiray YE, Ozkan AD, Elibol Z, Tekinay T (2012) Differential effects of nitrogen and sulfur deprivation on growth and biodiesel feedstock production of Chlamydomonas reinhardtii. Biotechnol Bioeng 109:1947–1957

Che R, Huang L, Yu X (2015) Enhanced biomass production, lipid yield and sedimentation efficiency by iron ion. Bioresour Technol 192:795–798

Chia MA, Lombardi AT, Melão MDGG, Parrish CC (2013) Effects of cadmium and nitrogen on lipid composition of Chlorella vulgaris (Trebouxiophyceae, Chlorophyta). Eur J Phycol 48:1–11

Chisti Y (2007) Biodiesel from microalgae. Biotechnol Adv 25:294–306

Concas A, Steriti A, Pisu M, Cao G (2014) Comprehensive modeling and investigation of the effect of iron on the growth rate and lipid accumulation of Chlorella vulgaris cultured in batch photobioreactors. Bioresour Technol 153:340–350

Demirbas MF (2011) Biofuels from algae for sustainable development. Appl Energy 88:3473–3480

Dlouhy AC, Outten CE (2013) The iron metallome in eukaryotic organisms. Met Ions Life Sci 12:241–278

Doubnerová V, Ryšlavá H (2011) What can enzymes of C4 photosynthesis do for C3 plants under stress? Plant Sci 180:575–583

Doyle JJ, Doyle JL (1987) A rapid DNA isolation procedure for small quantities of fresh leaf tissue. Phytochem Bull 19:11–15

Fan J, Andre C, Xu C (2011) A chloroplast pathway for the de novo biosynthesis of triacylglycerol in Chlamydomonas reinhardtii. FEBS Lett 585:1985–1991

Glaesener AG, Merchant SS, Blaby-Haas CE (2013) Iron economy in Chlamydomonas reinhardtii. Front Plant Sci 4:337

Glass JB, Wolfe-Simon F, Anbar AD (2009) Coevolution of metal availability and nitrogen assimilation in cyanobacteria and algae. Geobiology 7:100–123

Goncalves EC, Wilkie AC, Kirst M, Rathinasabapathi B (2016) Metabolic regulation of triacylglycerol accumulation in the green algae: identification of potential targets for engineering to improve oil yield. Plant Biotechnol J 14:1649–1660

Gouveia L, Oliveira AC (2009) Microalgae as a raw material for biofuels production. J Ind Microbiol Biotechnol 36:269–274

Griffiths MJ, Harrison STL (2009) Lipid productivity as a key characteristic for choosing algal species for biodiesel production. J Appl Phycol 21:493–507

Gris B, Morosinotto T, Giacometti GM, Bertucco A, Sforza E (2014) Cultivation of Scenedesmus obliquus in photobioreactors: effects of light intensities and light-dark cycles on growth, productivity, and biochemical composition. Appl Biochem Biotechnol 172:2377–2389

Hernández-Torres A, Zapata-Morales AL, Ochoa Alfaro AE, Soria-Guerra RE (2016) Identification of gene transcripts involved in lipid biosynthesis in Chlamydomonas reinhardtii under nitrogen, iron and sulfur deprivation. World J Microbiol Biotechnol 32:55

Hu Q, Sommerfeld M, Jarvis E, Ghirardi M, Posewitz M, Seibert M, Darzins A (2008) Microalgal triacylglycerols as feedstocks for biofuel production: perspectives and advances. Plant J 54:621–639

Huang X, Wei L, Huang Z, Yan JW (2014) Effect of high ferric ion concentrations on total lipids and lipid characteristics of

Tetraselmis subcordiformis, Nannochloropsis oculata and *Pavlova viridis*. J Appl Phycol 26:105–114

Illman AM, Scragg AH, Shales SW (2000) Increase in *Chlorella* strains calorific values when grown in low nitrogen medium. Enzym Microb Technol 27:631–635

Islam MA, Ayoko GA, Brown R, Stuart D, Heimann K (2013) Influence of fatty acid structure on fuel properties of algae derived biodiesel. Procedia Eng 56:591–596

Kadar E, Tarran GE, Jha AW, Al-Subiai SN (2011) Stabilisation of engineered zero-valent nanoiron with Na-acrylic copolymer enhances spermiotoxicity. Environ Sci Technol 45:3245–3251

Keenan C, Goth-Goldstein R, Lucas D, Sedlak LD (2009) Oxidative stress induced by zero-valent iron nanoparticles and Fe(II) in human bronchial epithelial cells. Environ Sci Technol 43:4555–4560

Kehrer JP (2000) The Haber-Weiss reaction and mechanisms of toxicity. Toxicology. 149:43–50

Knothe G (2012) Fuel properties of highly polyunsaturated fatty acid methyl esters. Prediction of fuel properties of algal biodiesel. Energy Fuel 26:5265–5273

Koller M, Muhr A, Braunegg G (2014) Microalgae as versatile cellular factories for valued products. Algal Res 6:52–63

Lang X, Dalai AK, Bakhshi NN, Reaney MJ, Hertz PB (2001) Preparation and characterization of bio-diesels from various bio-oils. Bioresour Technol 80:53–62

Lari Z, Moradi-kheibari N, Ahmadzadeh H, Abrishamchi P, Moheimani NR, Murry MA (2016) Bioprocess engineering of microalgae to optimize lipid production through nutrient management. J Appl Phycol 28:3235–3250

Li Y, Han D, Sommerfeld M, Hu Q (2011) Photosynthetic carbon partitioning and lipid production in the oleaginous microalga *Pseudochlorococcum* sp. (Chlorophyceae) under nitrogen-limited conditions. Bioresour Technol 102:123–129

Li-Beisson Y, Thelen JJ, Fedosejevs E, Harwood JL (2019) The lipid biochemistry of eukaryotic algae. Prog Lipid Res 74:31–68

Liu ZY, Wang GC, Zhou BC (2008) Effect of iron on growth and lipid accumulation in *Chlorella vulgaris*. Bioresour Technol 99:4717–4722

Marchetti A, Maldonado MT (2016) Iron. In: Borowitzka MA, Beardall J, Raven JA (eds) The physiology of microalgae. Springer, Dordrecht, pp 233–279

Mata TM, Martins AA, Caetano NS (2010) Microalgae for biodiesel production and other applications: a review. Renew Sustain Energy Rev 14(1):217–232

Miller GW, Huang IJ, Welkie GW, Pushnik JC (1995) Function of iron in plants with special emphasis on chloroplasts and photosynthetic activity. In: Abadía J (ed) Iron nutrition in soils and plants. Springer, Dordrecht, pp 19–28

Nascimento IA, Marques SSI, Cabanelas ITD, Pereira SA, Druzian JI, de Souza CO, Vich DV, de Carvalho GC, Nascimento MA (2013) Screening microalgae strains for biodiesel production: lipid productivity and estimation of fuel quality based on fatty acids profiles as selective criteria. Bioenergy Res 6:1–13

Osundeko O, Davis H, Pittman JK (2013) Oxidative stress-tolerant microalgae strains are highly efficient for biofuel feedstock production on wastewater. Biomass Bioenergy 56:284–294

Pádrová K, Lukavský J, Nedbalová L, Čejková A, Cajthaml T, Sigler K, Vítová M, Řezanka T (2015) Trace concentrations of iron nanoparticles cause overproduction of biomass and lipids during cultivation of cyanobacteria and microalgae. J Appl Phycol 27:1443–1451

Patil V, Tran KQ, Giselrød HR (2008) Towards sustainable production of biofuels from microalgae. Int J Mol Sci 9:1188–1195

Predojević Z, Škrbić B, Durišić-Mladenović N (2012) Transesterification of linoleic and oleic sunflower oils to biodiesel using CaO as a solid base catalyst. J Serb Chem Soc 77:815–832

Qiu R, Gao S, Lopez PA, Ogden KL (2017) Effects of pH on cell growth, lipid production and CO_2 addition of microalgae *Chlorella sorokiniana*. Algal Res 28:192–199

Rai MP, Gupta S (2016) Effect of media composition and light supply on biomass, lipid content and FAME profile for quality biofuel production *from Scenedesmus abundans*. Energy Convers Manag 141:85–92

Rodolfi L, Chini Zittelli G, Bassi N, Padovani G, Biondi N, Bonini G, Tredici MR (2009) Microalgae for oil: strain selection, induction of lipid synthesis and outdoor mass cultivation in a low-cost photobioreactor. Biotechnol Bioeng 1:100–112

Ruangsomboon S, Ganmanee M, Choochote S (2013) Effects of different nitrogen, phosphorus, and iron concentrations and salinity on lipid production in newly isolated strain of the tropical green microalga, *Scenedesmus dimorphus* KMITL. J Appl Phycol 25:867–874

Salamaa E, Kuradea MB, Abou-Shanabb RAI, El-Dalatonya MM, Yanga IS, Minc B, Jeona BH (2017) Recent progress in microalgal biomass production coupled with wastewater treatment for biofuel generation. Renew Sust Energ Rev 79:1189–1211

Schenk PM, Thomas-Hall SR, Stephens E, Marx UC, Mussgnug JH, Posten C, Olaf Kruse O, Hankamer B (2008) Second generation biofuels: high-efficiency microalgae for biodiesel production. Bioenergy Res 1:20–43

Shao Y, Fang H, Zhou H, Wang Q, Zhu Y, He Y (2017) Detection and imaging of lipids of *Scenedesmus obliquus* based on confocal Raman microspectroscopy. Biotechnol Biofuels 10:300

Sharma KK, Schuhmann H, Schenk PM (2012) High lipid induction in microalgae for biodiesel production. Energies 5:1532–1553

Shuba ES, Kifle D (2018) Microalgae to biofuels: 'promising' alternative and renewable energy, review. Renew Sust Energ Rev 81:743–755

Singh B, Guldhe A, Rawat A, Bux F (2014) Towards a sustainable approach for development of biodiesel from plant and microalgae. Bioresour Technol 102:57–70

Sivaramakrishnan R, Incharoensakdi A (2017) Enhancement of total lipid yield by nitrogen, carbon, and iron supplementation in isolated microalgae. J Phycol 53:855–868

Søndergaard M (2009) Redox potential. In: Likens GE (ed) Encyclopedia of inland waters. Academic Press, Oxford, pp 852–859

Stanier RY, Kunisawa R, Mandel M, Cohen-Bazire G (1971) Purification and properties of unicellular blue-green algae (Chroococcales). Bacteriol Rev 35:171–205

Stephenson AL, Dennis JS, Howe CJ, Scott SA, Smith AG (2010) Influence of nitrogen-limitation regime on the production by *Chlorella vulgaris* of lipids for biodiesel feedstocks. Biofuels 1:47–58

Sun X, Cao Y, Xu H, Liu Y, Sun JR, Qiao DR, Cao Y (2014) Effect of nitrogen-starvation, light intensity and iron on triacylglyceride/carbohydrate production and fatty acid profile of *Neochloris oleoabundans* HK-129 by a two-stage process. Bioresour Technol 155:204–212

Sunda WG, Price NM, Morel FMM (2005) Trace metal ion buffers and their use in culture studies. In: Andersen RA (ed) Algal culturing techniques. Elsevier, Amsterdam, pp 35–63

Tamura K, Stecher G, Peterson D, Filipski A, Kumar S (2013) MEGA6: molecular evolutionary genetics analysis version 6.0. Mol Biol Evol 30:2725–2729

Terauchi AM, Peers G, Kobayashi MC, Niyog KK, Merchant SS (2010) Trophic status of *Chlamydomonas reinhardtii* influences the impact of iron deficiency on photosynthesis. Photosynth Res 105:39–49

Urzica EI, Vieler A, Hong-Hermesdorf A, Page MD, Casero D, Gallaher SD, Kropat J, Pellegrini M, Benning C, Merchant SS (2013) Remodeling of membrane lipids in iron-starved *Chlamydomonas*. J Biol Chem 288:30246–30258

Wan M, Jin X, Xia J, Rosenberg JN, Yu G, Nie Z, Oyler GA, Betenbaugh MJ (2014) The effect of iron on growth, lipid accumulation, and

gene expression profile of the freshwater microalga *Chlorella sorokiniana*. Appl Microbiol Biotechnol 98:9473–9481

Wu H, Miao X (2014) Biodiesel quality and biochemical changes of microalgae *Chlorella pyrenoidosa* and *Scenedesmus obliquus* in response to nitrate levels. Bioresour Technol 170:421–427

Wu Y, Zhou S, Qin F, Zheng K, Ye X (2010) Modeling the oxidation kinetics of Fenton's process on the degradation of humic acid. J Hazard Mater 179:533–539

Xu Y, Boeing WJ (2014) Modeling maximum lipid productivity of microalgae: review and next step. Renew Sust Energ Rev 32:29–39

Yeesang C, Cheirsilp B (2011) Effect of nitrogen, salt, and iron content in the growth medium and light intensity on lipid production by microalgae isolated from freshwater sources in Thailand. Bioresour Technol 102:3034–3040

Zhao P, Gu W, Huang A, Wu S, Liu C, Huan L, Gao S, Xie X, Wa G (2018) Effect of iron on the growth of *Phaeodactylum tricornutum* via photosynthesis. J Phycol 54:34–43

Publisher's note   Springer Nature remains neutral with regard to jurisdictional claims in published maps and institutional affiliations.